

# Intrinsic self-rotation of BEC Bloch wave packets

Roberto B. Diener, Ganesh Sundaram, and Qian Niu  
*Department of Physics, The University of Texas, Austin, Texas 78712-1081*

Artem M. Dudarev  
*Department of Physics, The University of Texas, Austin, Texas 78712-1081 and  
 Center for Nonlinear Dynamics, The University of Texas, Austin, Texas 78712-1081*

The semiclassical theory of Bloch wave packet dynamics predicts a self-rotation angular momentum in asymmetric periodic potentials, which has never been observed. We show how this is manifested in Bose-Einstein condensed atoms in optical lattices. Displacing the wave packet to a corner of the Brillouin zone we obtain a current distribution with a non-quantized angular momentum, independent of the size of the distribution. A weak interatomic interaction does not modify the results, affecting only the rate of spreading in the lattice. A strong repulsive interaction results in a collapse of the wavefunction into matter-wave lattice solitons.

The semiclassical equations of motion for electrons in crystals have played a fundamental role in the theory of charge transport in metals and semiconductors [1]. Because of Berry phase and gradient corrections [2, 3], two striking effects occur for systems without time reversal or spatial inversion symmetry. The first one is a lateral displacement of the particles relative to the external force, and is responsible for the anomalous Hall effect in ferromagnets [4, 5]. The second one is the appearance of an orbital magnetization, due to the rotation of the wave packet around its center. This latter effect has received little attention and no experimental observation of it has been performed so far. In this letter we propose a demonstration of this wave packet self-rotation using ultracold atoms in optical lattices. Such a system has been employed in the past to exhibit a number of basic phenomena in condensed matter physics [6, 7].

A dual purpose of this work is to study the generation of novel matter-wave states using the knowledge gathered in electron transport theory. Bose-Einstein condensates can be manipulated experimentally with great precision [8] and the equation of motion for the condensate wavefunction in a periodic potential coincides with the one for electrons moving in a crystal. Several experimental studies of condensates in optical lattices have already been performed [9, 10]. The generation of states in an asymmetrical potential must take into consideration the two effects mentioned before.

The semiclassical description assumes that the wave function for a particle is a superposition of Bloch waves from a single band

$$|\Psi\rangle = \int_{BZ} d\mathbf{k} f(\mathbf{k}) |\Psi_{\mathbf{k}}\rangle, \quad (1)$$

in which the distribution  $f(\mathbf{k})$  is centered at a point  $\mathbf{k}_c$  in the Brillouin zone with a small dispersion  $\sigma_k$ . This in turn yields a spatial dispersion  $\sigma_r$  much larger than the size of a unit cell. The Bloch waves have the property that  $|\Psi_{\mathbf{k}}\rangle = e^{i\mathbf{k}\cdot\mathbf{r}}|u_{\mathbf{k}}\rangle$ , where  $u_{\mathbf{k}}(\mathbf{r})$  preserves the periodicity of the lattice potential  $V_{\text{latt}}(\mathbf{r})$ . These wave functions

are the solutions of the equation

$$\begin{aligned} \hat{H}_0(\mathbf{k})|u_n(\mathbf{k})\rangle &\equiv \left[\frac{1}{2M}(\mathbf{p} + \hbar\mathbf{k})^2 + V_{\text{latt}}(\mathbf{r})\right]|u_n(\mathbf{k})\rangle \\ &= \mathcal{E}_n(\mathbf{k})|u_n(\mathbf{k})\rangle. \end{aligned} \quad (2)$$

We restrict our study to a single band, thus dropping the band index  $n$  in what follows.

By defining the Lagrangian  $\mathcal{L}(\mathbf{k}_c, \mathbf{r}_c, \dot{\mathbf{k}}_c, \dot{\mathbf{r}}_c) = \langle\Psi|(i\hbar\frac{\partial}{\partial t} - \hat{H})|\Psi\rangle$  using as coordinates the position of the center of the wave packet in real and reciprocal space, we can find the equations of motion, which read

$$\begin{aligned} \dot{\mathbf{r}}_c &= \frac{1}{\hbar} \frac{\partial \mathcal{E}_S(\mathbf{k}_c)}{\partial \mathbf{k}_c} - \dot{\mathbf{k}}_c \times \boldsymbol{\Omega}(\mathbf{k}_c), \\ \hbar \dot{\mathbf{k}}_c &= -e\mathbf{E}(\mathbf{r}_c) - e\dot{\mathbf{r}}_c \times \mathbf{B}(\mathbf{r}_c). \end{aligned} \quad (3)$$

For atoms in an optical lattice, the “electric” and “magnetic” forces are the inertial Coriolis forces, if we describe the motion in a frame moving with the lattice which is linearly accelerated and/or rotated, respectively. Equation (4) is the Lorentz force equation found in any solid-state physics textbook, but (3) contains two corrections from the standard result. One is the presence of the Berry curvature, defined as

$$\boldsymbol{\Omega}(\mathbf{k}_c) = i\left\langle\frac{\partial u}{\partial \mathbf{k}_c}\right| \times \left|\frac{\partial u}{\partial \mathbf{k}_c}\right\rangle \quad (5)$$

(notice that this can be nonzero for complex  $u(\mathbf{r})$ ). It acts dynamically as the symmetrical analogue of the magnetic field if we exchange the  $\mathbf{r}_c$  and  $\mathbf{k}_c$  variables, and is related to the Hall effect in magnetic sub-bands [2] and the anomalous Hall effect in ferromagnets [4, 5]. The second correction is to the band energy, which contains a term proportional to the orbital magnetization energy,  $\mathcal{E}_S(\mathbf{k}_c) = \mathcal{E}(\mathbf{k}_c) + \frac{e}{2M}\mathbf{S}(\mathbf{k}_c) \cdot \mathbf{B}(\mathbf{r}_c)$ . This magnetization is proportional to the internal angular momentum of the wave packet, i.e.

$$\mathbf{S} = \int d\mathbf{r} (\mathbf{r} - \mathbf{r}_c) \times \mathbf{J}(\mathbf{r}), \quad (6)$$

where  $\mathbf{J}(\mathbf{r})$  is the current density [2]. In terms of the Bloch waves, it is given by

$$\mathbf{S}(\mathbf{k}_c) = i\frac{M}{\hbar} \left\langle \frac{\partial u}{\partial \mathbf{k}_c} \right| \times (H(\mathbf{k}_c) - \mathcal{E}(\mathbf{k}_c)) \left| \frac{\partial u}{\partial \mathbf{k}_c} \right\rangle. \quad (7)$$

As long as the semiclassical approximation holds, this result is independent of the distribution  $f(\mathbf{k})$  used, and hence of the width of the wave packet in real space. In particular it is independent of time for a fixed value of  $\mathbf{k}_c$ ; the wave packet maintains its angular momentum constant as it spreads on the lattice.

The reason that in most circumstances these corrections to the semiclassical equations of motion do not need to be taken into consideration is the constraints imposed on them by the symmetry of the Hamiltonian. If the system possesses time-reversal symmetry, then both vectors  $\boldsymbol{\Omega}$  and  $\mathbf{S}$  are odd functions of  $\mathbf{k}_c$ . On the other hand, if it possesses inversion symmetry then they are even functions of  $\mathbf{k}_c$ . This implies that in systems with both symmetries they vanish throughout the Brillouin zone.

We will consider a system of Bose-condensed atoms moving in an asymmetric two-dimensional optical lattice. The interaction between the atoms is neglected for the moment. In order to break inversion symmetry, we consider an asymmetric hexagonal lattice, as shown in Fig. 1(a). In the tight-binding regime, in which the potential wells denoted by blue color are deep, the atoms are located in the ground state of these wells. Since the calculations can be performed analytically in this case, we consider it first [11].

Let the on-site energies for sites A and B be  $\epsilon_A = \epsilon_g/2$  and  $\epsilon_B = -\epsilon_g/2$ , and the tunnelling matrix element be non-vanishing only between nearest neighbors with magnitude  $\hbar$ . The lattice is triangular, with basis vectors  $\mathbf{a}_1 = \sqrt{3}a\mathbf{e}_y$  and  $\mathbf{a}_2 = \frac{3}{2}a\mathbf{e}_x + \frac{\sqrt{3}}{2}a\mathbf{e}_y$ ; here  $a$  is the distance between nearest neighbors. Numbering the sites in the lattice by  $(m, n)$  such that  $\mathbf{R}_{m,n} = m\mathbf{a}_1 + n\mathbf{a}_2$ , we obtain the discrete Schrödinger equation for the eigenvectors of the Hamiltonian

$$\mathcal{E} \psi_{m,n}^A = \epsilon_A \psi_{m,n}^A - \hbar(\psi_{m,n+1}^B + \psi_{m,n}^B + \psi_{m+1,n}^B), \quad (8)$$

$$\mathcal{E} \psi_{m,n}^B = \epsilon_B \psi_{m,n}^B - \hbar(\psi_{m,n-1}^A + \psi_{m,n}^A + \psi_{m-1,n}^A). \quad (9)$$

The Bloch waves for this Hamiltonian are calculated by writing  $\psi_{m,n}^{A,B} = \phi^{A,B} \exp(i\mathbf{k} \cdot \mathbf{R}_{m,n})$ , with which we obtain

$$H(\mathbf{k}) = \begin{pmatrix} \epsilon_A & V(\mathbf{k}) \\ V(\mathbf{k})^* & \epsilon_B \end{pmatrix}. \quad (10)$$

The off-diagonal element is  $V(\mathbf{k}) = -\hbar(1 + e^{i\mathbf{k} \cdot \mathbf{a}_1} + e^{i\mathbf{k} \cdot \mathbf{a}_2})$ . The diagonalization of the Bloch Hamiltonian is straightforward, yielding the two energy bands

$$\mathcal{E}_{\pm}(\mathbf{k}) = \pm \sqrt{\left(\frac{\epsilon_g}{2}\right)^2 + |V(\mathbf{k})|^2}. \quad (11)$$

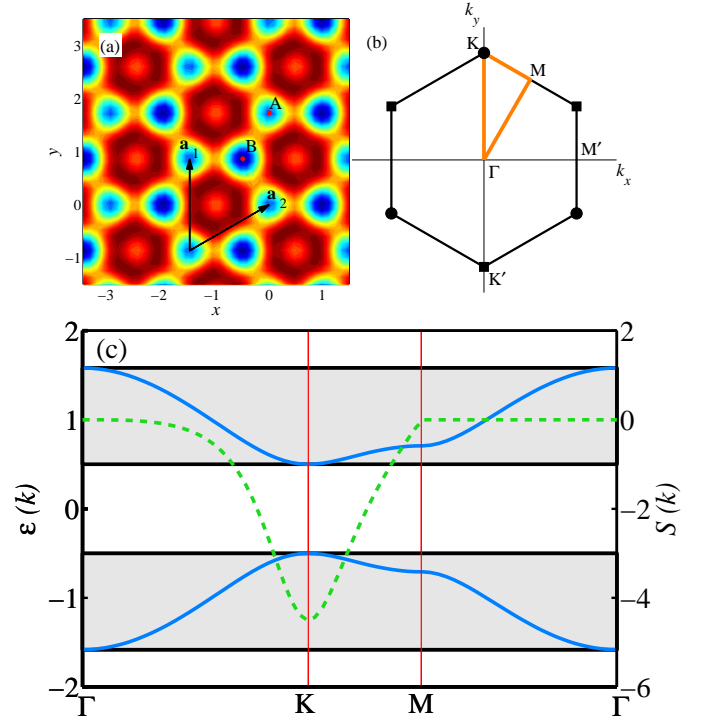


FIG. 1: (a) potential energy seen by the atoms; the blue color corresponds to the lowest values. In the tight-binding approximation, particles are localized in the A and B sites only. The corresponding Brillouin zone in reciprocal space is shown in (b); due to symmetry, all points marked by a circle correspond to the same K point. In (c) we show the band structure (solid line, left axis) and the angular momentum  $S$  (dashed line, right axis) for a tight binding band with  $\epsilon_g = \hbar$ .

The energy bands are depicted in Fig. 1(c). The bottom band has a minimum at the origin ( $\Gamma$  point) and a maximum at the K point,  $\mathbf{k}_0 = 4\pi/(3\sqrt{3}a)\mathbf{e}_y$ , at which  $V(\mathbf{k}_0) = 0$ . This is also the point of closest approach to the excited band, with the gap being equal to  $\epsilon_g$ .

For the ground state wave function,

$$\frac{\phi^A}{\phi^B} = -\frac{V(\mathbf{k})}{\mathcal{E}_+ + (\epsilon_g/2)}. \quad (12)$$

In two dimensional systems, the Berry curvature and the angular momentum are directed along the perpendicular,  $z$ -direction. Their values for the system are

$$\begin{aligned} \Omega(\mathbf{k}) &= \frac{\sqrt{3}\epsilon_g\hbar^2a^2}{16\mathcal{E}_+^3} [\sin(\sqrt{3}k_ya) - 2\sin(\sqrt{3}k_ya/2)\cos(3k_xa/\sqrt{3})] \\ S(\mathbf{k}) &= \frac{M}{\hbar}(2\mathcal{E}_+)\Omega(\mathbf{k}). \end{aligned} \quad (14)$$

An intriguing relation at the K point, where  $S$  is minimum, is

$$S(\mathbf{k}_0) = \hbar \frac{M}{M^*} \quad (15)$$

where  $M^*$  is the effective mass, given by  $M^* = -2\epsilon_g \hbar^2 / (9h^2 a^2)$ .

The angular momentum  $S$  is plotted in reciprocal space in figure 1(c) (dashed green line). From (14) we see that the dependence of the Berry curvature on quasimomentum in reciprocal space is very similar. In particular, both of these quantities attain their maximum absolute value at  $\mathbf{k}_0$  and all symmetrically located points. The value attained diverges as the gap size  $\epsilon_g$  goes to zero. Notice that the angular momentum is not quantized.

The angular momentum that we have calculated is the total value for the wave packet. To study its distribution in real space, we consider a Gaussian distribution of Bloch waves around the point  $\mathbf{k}_0$ , i.e.

$$f(\mathbf{k}) = \frac{1}{\sqrt{\pi}\sigma_k} e^{-\frac{(\mathbf{k}-\mathbf{k}_0)^2}{2\sigma_k^2}}. \quad (16)$$

In figure 2(a) we show the distribution of currents as a function of position, which show a clear rotating pattern. This distribution of currents is not the one found near a vortex, for which the currents diverge at the center. Approximating the off-diagonal term in the Bloch Hamiltonian near  $\mathbf{k}_0$  as

$$V(\mathbf{k}) \approx \frac{3ta}{2} e^{i7\pi/6} ((k_x - k_{0,x}) + i(k_y - k_{0,y})), \quad (17)$$

we can calculate the wave function coefficients as

$$\psi_{m,n}^B \approx 2\sqrt{\pi}\sigma_k e^{i\mathbf{k}_0 \cdot \mathbf{R}_{m,n}} e^{-R_{m,n}^2 \sigma_k^2 / 2}, \quad (18)$$

$$\psi_{m,n}^A \approx \frac{ta\sigma_k^2}{\epsilon_g} e^{i2\pi/3} (R_{m,n,x} + iR_{m,n,y}) \psi_{m,n}^B. \quad (19)$$

Notice that the probability for B sites has a maximum at the center of the wave packet, while the probability for A sites is zero there. This is related to the fact that for a single Bloch wave at  $\mathbf{k}_0$  the A sites are completely depopulated, and it is only through the presence of a distribution of Bloch waves that some of the A sites acquire some density. The distribution of A sites has a maximum when  $R_{m,n} \approx 1/\sigma_k$ . Since the currents depend on the values at neighboring sites, it is at this distance that the currents are maximized.

In a real experiment, the atoms will move in an optical lattice generated by counterpropagating laser beams or a holographic method, in which the potential is generated with a phase or amplitude mask [12]. The potential to be chosen can be obtained by calculating the Fourier transform of a sum of Gaussian wells located at the A and B sites and keeping the largest terms. The potential obtained is of the form

$$\begin{aligned} V_{\text{latt}}(\mathbf{r}) = & V_0 [\cos((\mathbf{k}_1 - \mathbf{k}_2) \cdot \mathbf{r}) + \cos((2\mathbf{k}_1 + \mathbf{k}_2) \cdot \mathbf{r}) \\ & + \cos((2\mathbf{k}_2 + \mathbf{k}_1) \cdot \mathbf{r})] \\ & + V_1 [\cos(\mathbf{k}_1 \cdot \mathbf{r} + \alpha) + \cos(\mathbf{k}_2 \cdot \mathbf{r} + \alpha) \\ & + \cos((\mathbf{k}_1 + \mathbf{k}_2) \cdot \mathbf{r} - \alpha)]. \end{aligned} \quad (20)$$

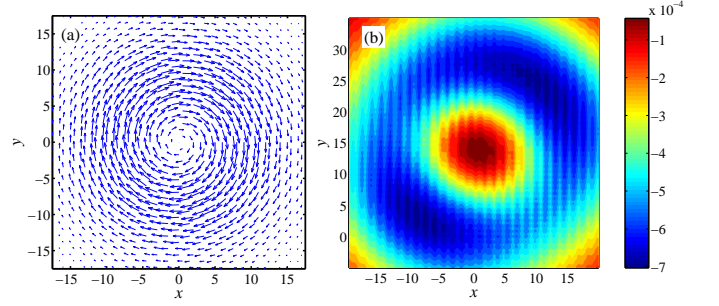


FIG. 2: (a): distribution of currents in the tight-binding limit for a wave packet centered at  $\mathbf{k}_0$ . (b): calculation of the averaged angular momentum distribution for atoms in the periodic potential (20) with  $V_0 = -4$ ,  $V_1 = 4.664$  after the wave packet has been displaced to  $\mathbf{k}_0$ . The averaging assumes an experimental precision in position of  $\sigma_{\text{inst}} = a$ .

Here the wavevectors are  $\mathbf{k}_1 = -\frac{2\pi}{3a}\mathbf{e}_x + \frac{2\pi}{\sqrt{3}a}\mathbf{e}_y$ , and  $\mathbf{k}_2 = \frac{4\pi}{3a}\mathbf{e}_x$ . We will use a system of units in which  $\hbar = M = a = 1$ . It is worth noticing that the ratio between the two amplitudes  $V_1$  and  $V_0$  controls the widths of the gaussian potentials located at the lattice sites, while the phase yields the ratio between the depths of the potentials. For the symmetric potential,  $\alpha = \pi/3$ . In our calculations we have used a value of  $\alpha = 1.1$ .

A wave packet of the form (1) at  $\mathbf{k}_c = 0$  in the lowest energy band of a periodic potential can be obtained starting with a Gaussian wave packet in real space (e.g. the ground state of a harmonic trap) and adiabatically turning on the lattice [14]. The study of the angular momentum as a function of the quasimomentum of the wave packet can be performed by applying an “electric” field (see Eq. (4)), which in the case of cold atoms corresponds to an acceleration of the lattice. The atoms are displaced in reciprocal space along the direction of the acceleration, while they perform Bloch oscillations in real space.

The calculated motion of the wave packet in real space and its angular momentum as a function of time are shown in Fig. 3. The wave packet starts at I, moving against the direction of the acceleration. As the quasimomentum reaches the K point in reciprocal space (II in real space), the Berry curvature displaces the distribution to the right, and the angular momentum achieves its smallest value. The averaged distribution of the angular momentum is shown in the right panel of Fig. 2, which agrees with the result for the tight-binding model (left panel of the same figure). Eventually, the wave packet reaches point III, where it shows no rotation and starts retracing its path. When it reaches II again, it possesses a maximum (positive) angular momentum, which it loses once it comes back to I.

The velocity distribution of the atoms (from which the angular momentum of the wave packet can be calculated) can be measured by Doppler-sensitive Raman transitions [13]. In this way, atoms with a selected veloc-

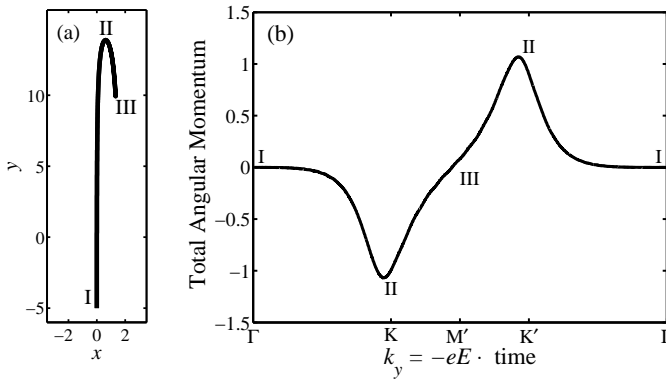


FIG. 3: (a): motion in real space of the center of the wave packet. (b): angular momentum as a function of the position in reciprocal space, calculated for an “electric” field of  $-eE = 0.05$  applied along the  $y$ -direction.

ity are driven to a dark state, and one can get rid of the rest of the atoms by shining resonant light. Imaging the remaining atoms, one may obtain the real space distribution of atoms with the given velocity. By changing the detuning, different sets of atoms are observed. Another observable result in this case is the motion caused by the anomalous velocity (due to the nonvanishing Berry curvature). This displaces the center of the wave packet by an amount equal to

$$\Delta \mathbf{r}_c = - \int_0^{\mathbf{k}} d\mathbf{k}' \times \boldsymbol{\Omega}(\mathbf{k}'), \quad (21)$$

an amount independent of the magnitude of the driving  $-eE$  field.

Care must be taken in the experiment not to excite the atoms to a higher energy band while the lattice is accelerated. The largest probability for this to happen occurs when the wave packet is at  $\mathbf{k}_0$ , where the gap between the two bands is smallest and the particles can undergo Landau-Zener tunnelling. The probability for this to happen is proportional to  $\exp(-\epsilon_g^2/|eE|)$ , therefore the electric field must satisfy  $|eE| \ll \epsilon_g^2$ .

One has to be careful in the design of the lattice in which the rotation is observed in order to make a direct comparison with the tight-binding model. Using a potential depth  $V_0$  much smaller than the one we used in the simulations one has to include the probability of atoms tunnelling to a non-nearest neighbor. These currents between B sites would not add to the total angular momentum in the wave packet but can yield a much more complicated distribution of currents.

We finally comment on the consequences of adding the interatomic interaction between the particles. The interaction corresponds to the addition of terms  $g|\psi_{m,n}|^2\psi_{m,n}$  in the right hand sides of (8) and (9). For weak interaction strength we observe no change in the values of the angular momentum at  $\mathbf{k}_0$ , which remains constant in

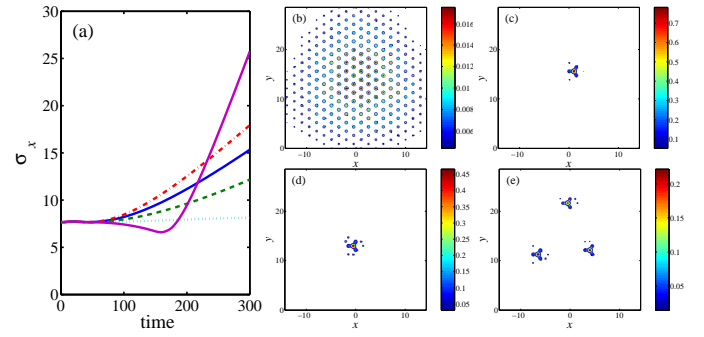


FIG. 4: (a) Dispersion of the wave packet with time for different values of the interaction strength in the tight-binding limit ( $\epsilon_g = 6$ ,  $t = 1$ ). The wave packet is accelerated from the  $\Gamma$  point to the  $K$  point, where the interaction strength is adiabatically increased. The lines correspond to  $g = 0$  (blue line),  $g = -1$  (red line),  $g = 1$  (green line),  $g = 1.9$  (cyan line), and  $g = 3$  (magenta line). In this last case, part of the wave packet collapses to a soliton when the size of the wave packet is minimum, with the remaining part diffusing at a fast rate afterwards. (b)-(e) show the wave function in real space after dispersing in the lattice for  $t \approx 200$ ; the interaction strengths are  $g = 1.5$  (b),  $g = 7.5$  (c),  $g = 15$  (d), and  $g = 30$  (e).

time. The rate of dispersion of the wave packet is modified, with a repulsive interaction ( $g > 0$ ) slowing down the dispersion and an attractive interaction ( $g < 0$ ) accelerating it (see Fig. 4). This counterintuitive result is related to the negative effective mass associated with particles near the top of the energy band [15]. Moreover, for repulsive interactions larger than a critical value, the system exhibits collapse into one or more breathing solitons [16]. These can be related to solitons in the gap between the two bands [17] similar to recently observed two dimensional optical solitons [18] and will be considered in a separate article.

The authors would like to acknowledge discussions with Mark G. Raizen.

- 
- [1] N. W. Ashcroft and N. D. Mermin, *Solid State Physics* (Saunders, Philadelphia, 1976).
  - [2] Ming-Che Chang and Qian Niu, Phys. Rev. B **53**, 7010 (1996).
  - [3] Ganesh Sundaram and Qian Niu, Phys. Rev. B **59**, 14915 (1999).
  - [4] T. Jungwirth, Q. Niu, and A. H. MacDonald, Phys. Rev. Lett. **88**, 207208 (2002).
  - [5] D. Culcer, A. H. MacDonald, and Q. Niu, to appear in Phys. Rev. B.
  - [6] M. Ben Dahan, E. Peik, J. Reichel, Y. Castin, and C. Salomon, Phys. Rev. Lett. **76**, 4508 (1996).
  - [7] Q. Niu, X.-G. Zhao, G. A. Georgakis, and M. G. Raizen, Phys. Rev. Lett. **76**, 4504 (1996); S. R. Wilkinson, C. F. Barucha, K. W. Madison, Q. Niu, and M. Raizen, Phys. Rev. Lett. **76**, 4512 (1996).

- [8] C. J. Pethick and H. Smith, *Bose-Einstein Condensation in Dilute Gases* (Cambridge University Press, Cambridge, 2002).
- [9] B. P. Anderson and M. A. Kasevich, *Science* **282**, 1686 (1998).
- [10] M. Greiner et al., *Nature (London)* **415**, 39 (2002).
- [11] Ganesh Sundaram, Doctoral Thesis, University of Texas at Austin (2000).
- [12] E. R. Dufresne, G. C. Spalding, M. T. Dearing, S. A. Sheets, and D. G. Grier, *Rev. Sci. Instr.* **72**, 1810 (2001).
- [13] M. Kasevich and S. Chu, *Phys. Rev. Lett.* **69**, 1740 (1992).
- [14] The condition to remain in the ground state can be estimated as  $t_{\text{turn on}} \gg 1/\Delta\mathcal{E}$ , where  $\Delta\mathcal{E}$  is the smallest excitation energy at  $\mathbf{k} = 0$  as the potential is turned on.
- [15] H. Pu, L. O. Baksmaty, W. Zhang, N. P. Bigelow, and P. Meystre, *Phys. Rev. A* **67**, 043605 (2003).
- [16] P. L. Christiansen, Yu. B. Gaididei, K. O. Rasmussen, V. K. Nezebtsev, and J. Juul Rasmussen, *Phys. Rev. B* **54**, 900 (1996).
- [17] E. A. Ostrovskaya, and Y. S. Kivshar, *Phys. Rev. Lett.* **90**, 160407 (2003).
- [18] J. W. Fleischer, M. Segev, N. K. Efremidis, and D. N. Christoulides, *Nature* **422**, 147 (2003); J. W. Fleischer, T. Carmon, M. Segev, N. K. Efremidis, and D. N. Christoulides, *Phys. Rev. Lett.* **90**, 023902 (2003).